Research Update: Enhanced energy storage density and energy efficiency of epitaxial Pb0.9La0.1(Zr0.52Ti0.48)O3 relaxor-ferroelectric thin-films deposited on silicon by pulsed laser deposition

Minh D. Nguyen, Evert P. Houwman, Matthijn Dekkers, Chi T. Q. Nguyen, Hung N. Vu, and Guus Rijnders

Citation: APL Mater. **4**, 080701 (2016); doi: 10.1063/1.4961636
View online: http://dx.doi.org/10.1063/1.4961636
View Table of Contents: http://scitation.aip.org/content/aip/journal/aplmater/4/8?ver=pdfcov
Published by the AIP Publishing

Articles you may be interested in

Challenges in the stoichiometric growth of polycrystalline and epitaxial PbZr0.52Ti0.48O3/La0.7Sr0.3MnO3 multiferroic heterostructures using pulsed laser deposition
J. Appl. Phys. **112**, 064101 (2012); 10.1063/1.4751027

Correlation between domain evolution and asymmetric switching in epitaxial Pb (Zr 0.52 Ti 0.48) O 3 thin films
Appl. Phys. Lett. **86**, 072904 (2005); 10.1063/1.1866506

Interface-oxygen-loss-controlled voltage offsets in epitaxial Pb (Zr 0.52 Ti 0.48) O 3 thin-film capacitors with La 0.7 Sr 0.3 Mn O 3 electrodes
Appl. Phys. Lett. **85**, 5013 (2004); 10.1063/1.1827929

Effect of oxygen stoichiometry on the ferroelectric property of epitaxial all-oxide La 0.7 Sr 0.3 MnO 3 /Pb(Zr 0.52 Ti 0.48)O 3 /La 0.7 Sr 0.3 MnO 3 thin-film capacitors
J. Vac. Sci. Technol. A **18**, 2412 (2000); 10.1116/1.1288195

Low-temperature growth of epitaxial LaNiO 3 / Pb(Zr 0.52 Ti 0.48) O 3 / LaNiO 3 on Si(001) by pulsed-laser deposition
J. Vac. Sci. Technol. A **18**, 79 (2000); 10.1116/1.582121

Pure Metals • Ceramics
Alloys • Polymers
in dozens of forms
Goodfellow
Small quantities *fast* • Expert technical assistance • 5% discount on online orders

Reuse of AIP Publishing content is subject to the terms at: https://publishing.aip.org/authors/rights-and-permissions. Download to IP: 130.89.45.232 On: Wed, 05 Oct 2016 09:44:39

APL MATERIALS **4**, 080701 (2016)

Research Update: Enhanced energy storage density and energy efficiency of epitaxial $Pb_{0.9}La_{0.1}(Zr_{0.52}Ti_{0.48})O_3$ relaxor-ferroelectric thin-films deposited on silicon by pulsed laser deposition

Minh D. Nguyen,[1,2,3,a] Evert P. Houwman,[1] Matthijn Dekkers,[2]
Chi T. Q. Nguyen,[3,4] Hung N. Vu,[3] and Guus Rijnders[1]
[1]*MESA+ Institute for Nanotechnology, University of Twente, P.O. Box 217, 7500AE Enschede, The Netherlands*
[2]*Solmates B.V., Drienerlolaan 5, 7522NB Enschede, The Netherlands*
[3]*International Training Institute for Materials Science, Hanoi University of Science and Technology, Dai Co Viet 1, Hanoi 10000, Vietnam*
[4]*Vietnam National University of Forestry, Chuong My district, Hanoi 10000, Vietnam*

(Received 16 June 2016; accepted 14 August 2016; published online 22 August 2016)

$Pb_{0.9}La_{0.1}(Zr_{0.52}Ti_{0.48})O_3$ (PLZT) relaxor-ferroelectric thin films were grown on $SrRuO_3/SrTiO_3/Si$ substrates by pulsed laser deposition. A large recoverable storage density (U_{reco}) of 13.7 J/cm^3 together with a high energy efficiency (η) of 88.2% under an applied electric field of 1000 kV/cm and at 1 kHz frequency was obtained in 300-nm-thick epitaxial PLZT thin films. These high values are due to the slim and asymmetric hysteresis loop when compared to the values in the reference undoped epitaxial lead zirconate titanate $Pb(Zr_{0.52}Ti_{0.48})O_3$ ferroelectric thin films (U_{reco} = 9.2 J/cm^3 and η = 56.4%) which have a high remanent polarization and a small shift in the hysteresis loop, under the same electric field. © *2016 Author(s). All article content, except where otherwise noted, is licensed under a Creative Commons Attribution (CC BY) license (http://creativecommons.org/licenses/by/4.0/).*
[http://dx.doi.org/10.1063/1.4961636]

Dielectric materials with high energy-storage density and high efficiency are greatly needed for the potential application in advanced pulse power capacitors for electronics and electrical power systems (the definitions of energy-storage density and efficiency of electrical energy storage capacitor devices are given in the supplementary material). Based on the physical principals, the materials with higher saturated polarization, smaller remanent polarization, and higher electrical breakdown field are the most promising candidates.[1] Most of the current studies on dielectric materials focus on paraelectric (linear dielectrics, DE), ferroelectric (FE), and antiferroelectric (AFE) materials. Recent studies indicate that the capacitors based on AFE materials offer dramatic improvement in energy storage density because of their high saturation polarization and negligible net spontaneous polarization, when compared to the DE and FE materials. Ahn *et al.*[2] reported on a very large recoverable energy storage density of 14.6 J/cm^3 and high energy efficiency of 91.3% under an electric field of 1000 kV/cm and at 1 kHz in polycrystalline $Pb_{0.97}Y_{0.02}[(Zr_{0.6}Sn_{0.6})_{0.925}Ti_{0.075}]O_3$ (PYZST) antiferroelectric thin film capacitors. The U_{reco} value of the PYZST film is similar to the values measured for other AFE films such as $PbZrO_3$ (U_{reco} = 13.3 J/cm^3),[3] $Pb_{0.95}Sr_{0.05}ZrO_3$ (U_{reco} = 14.5 J/cm^3),[4] and $Pb_{0.97}La_{0.02}(Zr_{0.98}Ti_{0.02})O_3$ (U_{reco} = 13.3 J/cm^3),[5] but the efficiency value of this PYZST film is much higher than that of the other AFE films.

Recently relaxor-ferroelectric (RFE) materials based on lanthanum-doped $Pb(Zr,Ti)O_3$ (PLZT) were also considered as a potential candidate for use in pulse power applications. Generally, the c/a ratio of the unit cell of such a material decreases to near unity, approaching a pseudocubic

[a]E-mail: d.m.nguyen@utwente.nl

 ©Author(s) 2016.

Reuse of AIP Publishing content is subject to the terms at: https://publishing.aip.org/authors/rights-and-permissions. Download to IP: 130.89.45.232 On: Wed, 05 Oct 2016 09:44:39

structure for high concentrations of lanthanum (La, ≥7%) in $Pb(Zr_{0.52}Ti_{0.48})O_3$ (PZT), which leads to relaxor behavior in PLZT.[6] The doping with La decreases the lead content and enhances the energy storage density in comparison to undoped PZT. Hao *et al.*[5] reported a high energy storage density of about 11.5 J/cm^3 and an energy efficiency of about 52.5%, measured under an electric field of 1000 kV/cm and at 1 kHz frequency, in relaxor-ferroelectric $Pb_{0.91}La_{0.09}(Ti_{0.65}Zr_{0.35})O_3$ thin films deposited on $Pt/Ti/SiO_2/Si$ (Pt/Si) with a sol-gel method; Tong *et al.*[7] studied relaxor-ferroelectric $Pb_{0.92}La_{0.08}(Ti_{0.52}Zr_{0.48})O_3$ films, also deposited by a sol-gel method on Pt/Si and $LaNiO_3/Ni$ (LNO/Ni), and achieved U_{reco} and η values of about 9.8 J/cm^3 and 55.0%, respectively, for 1 μm-thick film on Pt/Si, and about 12.0 J/cm^3 and 70.0% for a 1 μm-thick film on LNO/Ni (at 1000 kV/cm and 1 kHz). In Ref. 6, the energy storage properties of a series of sol-gel prepared samples of 8% La-doped PLZT films with varying Zr/Ti ratio were studied. Maximum energy storage density (about 13 J/cm^3 at 1000 kV/cm) and efficiency (78%) were found for the La-doped Morphotropic Phase Boundary (MPB) composition $Pb_{0.92}La_{0.08}Zr_{0.52}Ti_{0.48}O_3$.

Another route is the use of relaxor-ferroelectric superlattices as was done by Ortega *et al.*[8] In a 0.6 μm thick $BaTiO_3/Ba_{0.3}Sr_{0.7}TiO_3$ superlattice U_{reco} = 12.24 J/cm^3 at 1650 kV/cm was obtained and they extrapolated their results to 46 J/cm^3 at 5000 kV/cm, slightly below the breakdown voltage of the stack. However no efficiencies were quoted, but considering the fairly open hysteresis loops presented, these should be fairly moderate.

Although the recoverable energy storage densities in relaxor-ferroelectric PLZT films are comparable to those of antiferroelectric films, the above mentioned energy efficiencies are still significantly lower. Therefore further studies are needed to investigate the possibilities to improve the energy efficiency of relaxor ferroelectric films. Here, we demonstrate a large recoverable energy storage density (13.7 J/cm^3) and high energy efficiency (88.2%) at 1000 kV/cm in 300-nm-thick epitaxial $Pb_{0.9}La_{0.1}(Zr_{0.52}Ti_{0.48})O_3$ (PLZT) relaxor-ferroelectric thin films with $SrRuO_3$ (SRO) oxide electrodes on buffered $SrTiO_3/Si$ (STO/Si) substrates, fabricated by pulsed laser deposition (PLD). The La-doping causes a significant shift and slim polarization-hysteresis (*P-E*) loop of the epitaxial PLZT films as compared to that of the undoped epitaxial $Pb(Zr_{0.52}Ti_{0.48})O_3$ (PZT) films, maximizing the recoverable energy storage density (U_{reco}) and reducing the energy loss density (U_{loss}) significantly.

In this paper, $Pb(Zr_{0.52}Ti_{0.48})O_3$ (PZT) and $Pb_{0.9}La_{0.1}(Zr_{0.52}Ti_{0.48})O_3$ (PLZT) thin films were deposited on $SrRuO_3/SrTiO_3/Si$ substrates using a pulsed laser deposition (PLD) method. The MPB composition was based on the results of Hu *et al.*[6] The 8-nm-thick epitaxial $SrTiO_3$ (STO) buffer layer was grown by reactive molecular-beam epitaxy on Si substrates and acts as a seed layer for highly (001)-oriented growth of the subsequent perovskite layers.[9] The optimized deposition conditions of the PZT and PLZT thin films were laser repetition rate 10 Hz, energy density 2.5 J/cm^2, oxygen pressure 0.1 mbar, and substrate temperature 600 °C.[10] For the top and bottom $SrRuO_3$ (SRO) electrodes, the conditions were laser repetition rate 4 Hz, energy density 2.5 J/cm^2, oxygen pressure 0.13 mbar, and substrate temperature 600 °C. The thicknesses of the PZT and PLZT films are about 300 nm, while the top and bottom SRO electrodes are 100 nm.

Crystallographic properties of the PZT and PLZT thin films were analyzed by x-ray θ-2θ scans (XRD) and phi-scans (ϕ) using a PANalytical *X-ray* diffractometer. For electrical measurements, 200×200 μm^2 capacitors were patterned with a standard photolithography process and structured by argon-beam etching of the top-electrodes and wet-etching (HF-HCl solution) of the PZT and PLZT films. The polarization hysteresis loop measurements were performed with the ferroelectric mode of the aixACCT TF-2000 analyzer at 1 kHz and ±200 kV/cm amplitude. The polarization-switching cycle measurements were performed with a rectangular, bipolar switching pulse of 100 kV/cm pulse height and 5 μs pulse width at 100 kHz repetition frequency, while the *P-E* loops were measured again up to ±200 kV/cm and at 1 kHz frequency. A Süss MicroTech PM300 manual probe station equipped with a Keithley 4200 semiconductor characterization system was used for the capacitance measurement. The capacitance-electric field (*C-E*) curves were measured up to a *dc*-electric field of ±200 kV/cm and with a 1 kHz frequency *ac*-electric field with 3.3 kV/cm amplitude. The corresponding dielectric constants were calculated from the *C-E* curves. All measurements were performed at room temperature.

Reuse of AIP Publishing content is subject to the terms at: https://publishing.aip.org/authors/rights-and-permissions. Download to IP: 130.89.45.232 On: Wed, 05 Oct 2016 09:44:39

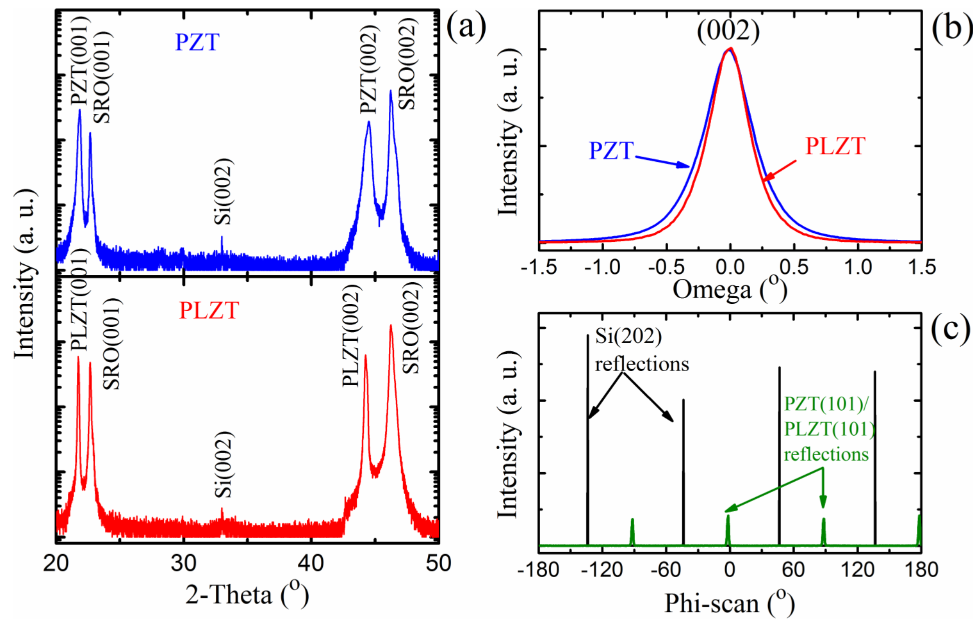

FIG. 1. (a) X-ray diffraction patterns and (b) rocking curves of the PZT and PLZT thin films deposited by pulsed laser deposition on SRO/STO/Si substrates. The full-widths at half maximum (FWHM) values are 0.45° and 0.38°, respectively, for the (002) peak positions of PZT and PLZT thin films. (c) X-ray ϕ-scan patterns of PZT{101}and PLZT{101} reflections.

Fig. 1(a) shows the x-ray θ-2θ patterns of the PZT and PLZT thin films deposited on the SRO electrodes buffered STO/Si substrates. This figure indicates that all films have a *c*-axis orientation. To clarify the in-plane orientation relation, phi-scan measurements were performed. The results shown in Fig. 1(c) demonstrate that the PZT (and PLZT) films are grown epitaxially on the SRO/STO/Si substrates. A 45° shift of the PZT{101} (and PLZT{101}) reflections with respect to the Si{202} reflections with a fourfold rotational symmetry is found, indicating that the PZT unit cells are rotated in-plane over 45° with respect to the Si lattice. The full-widths at half maximum ($FWHM_{\omega}$) of the rocking curves of the PZT(002) and PLZT(002) peaks in Fig. 2(b) were 0.45° and 0.38°, respectively, indicating a good crystalline quality of the PZT and PLZT films. The width of the rocking curves is a measure of the range over which the lattice structure in the different grains tilts with respect to the film normal[11] and is therefore an indication of the homogeneity of the films.

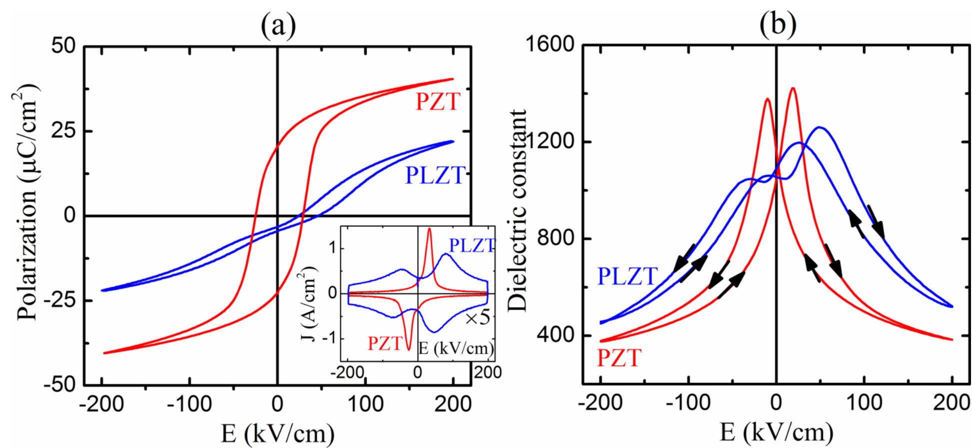

FIG. 2. (a) Bipolar ferroelectric P-E hysteresis loops and switching currents (inset) of the PLZT and PZT thin films performed. (b) Dielectric constant-electric field loops of the PLZT and PZT thin films.

Reuse of AIP Publishing content is subject to the terms at: https://publishing.aip.org/authors/rights-and-permissions. Download to IP: 130.89.45.232 On: Wed, 05 Oct 2016 09:44:39

Fig. 2(a) shows the initial ferroelectric (P-E) hysteresis loops recorded for the SRO/PZT/SRO and SRO/PLZT/SRO thin-film. The P-E loop of the PZT film displays a typical ferroelectric behavior with a saturation polarization (P_s) of 31.2 μC/cm^2 and a remanent polarization (P_r) of 21.6 μC/cm^2. Previous studies have indicated that the shape of the P-E loop becomes slimmer and slanted with increasing La concentration in the PZT films.[12] This is attributed to the reduction of the tetragonality of the PLZT unit cell with increasing La content, leading to a decrease in spontaneous polarization in the unit cell.[13] Also the number of Pb-vacancies increases with increasing La concentration, increasing the domain wall pinning and thus preventing domain switching, with the result that both P_r and P_s values are decreased.[13] Indeed also in this study, both of the above values in the PLZT film are found to be much lower than those in the PZT film. Second, the P-E loop of the 10% La-doped PLZT film shows a very large positive field shift (self-bias field $E_{sb} = (E_{c+} + E_{c-})/2$) of 34.6 kV/cm (for a positive voltage on the top electrode with respect to the bottom electrode, the externally applied field is directed top-to-bottom in the piezoelectric film, while a positive self-bias field—right-shift of the P-E loop—which corresponds to an internal built-in field directed bottom-to-top). On the other hand, the P-E loop of the undoped PZT film shows only a small shift (E_{sb} = 2.1 kV/cm). Third, the P-E loop of PLZT film shows some pinching of the loop at low fields, which is a characteristic of antiferroelectricity, hence it appears that in this sample, the relaxor material PLZT contains an antiferroelectric component, as shown in Fig. S1.

The switching current of the PZT, given in the inset of Fig. 2(a), shows only one peak when the ferroelectric domains are switched, while for the PLZT film two peaks appear. The peak associated with switching of the ferroelectric domains in the PLZT film appears at higher electrical fields than for the PZT film. The second peak in the switching current at the opposite direction of electric field is attributed to what seems to be an antiferroelectric phase, present in this film. The presence of this non-ferroelectric phase in PLZT film can also be seen in the dielectric constant-electric field curve (Fig. 2(b)), showing a double peak, whereas the well-defined loop of a normal ferroelectric is observed for the PZT film. A similar pinching of the P-E loop and double-peaked switching current loop is observed for the PLZT device on a SRO/CeO_2/YSZ/Si substrate, indicating also AFE behaviour (see supplementary material). The AFE behavior appears to be related to the crystalline quality of the bottom SRO/PLZT interface. In analogy with previous experiments with the growth of thin PZT layers on STO (Ref. 14) we expect that in the case of the STO/Si substrate the SRO grows epitaxially strained to the (relaxed) STO, adopting its in-plane lattice parameter. The initial growth layer of the PLZT starts to grow epitaxially compressively strained to the SRO/STO/Si, but relaxes within a few nm (possibly up to about 10 nm as in Ref. 14) to its bulk value, by defect incorporation. We assume that the compressive-in-plane strain induces an AFE state in the initial growth layer, while the largest, relaxed part of the film has the normal relaxor character.

Thus both PLZT films are deposited by PLD and are to a high degree single crystalline with initial lattice matching at the bottom electrode. On the other hand, the films made by constant speed drive (CSD) are polycrystalline with many defects and are therefore nearly fully strain relaxed, to the extent that no AFE can be induced by strain. This explanation suggests that the induced AFE layer is present at the bottom electrode interface, while the remainder of the film is in the relaxor phase.

Figs. 3(a) and 3(b) show the positive P-E loops of the PLZT and PZT thin films for different maximum electric field values (the bipolar P-E loops of the PLZT and PZT thin films are illustrated in Fig. S3). The maximum polarization (P_{max}) increases gradually as the applied electric field (E_{appl}) increases, whereas the remanent polarization (P_r) becomes only slightly larger or even remains constant (see Figs. 3(c) and 3(d)). The difference ($P_{max} - P_r$) is enhanced with increasing E_{appl} due to the larger increase of P_{max} with E_{appl} than of P_r. A high ($P_{max} - P_r$) value is beneficial for a high recoverable energy storage density value.

Fig. 4 shows the electric field–dependent recoverable energy storage density U_{reco} and energy efficiency η of the epitaxial-ferroelectric PZT and epitaxial-relaxor-ferroelectric PLZT thin films. The values of U_{reco} and η were calculated from the polarization on positive electric field in Fig. S2 using Equations (S1)-(S4). The U_{reco} values of PZT and PLZT thin films raise from 0.5 to 9.2 J/cm^3 and from 0.8 to 13.7 J/cm^3, respectively, as E_{appl} is increased from 100 to 1000 kV/cm (Fig. 4(a)). As shown in Fig. 4(b), in this measurement range, the η value of PLZT film varies between 83.5%

Reuse of AIP Publishing content is subject to the terms at: https://publishing.aip.org/authors/rights-and-permissions. Download to IP: 130.89.45.232 On: Wed, 05 Oct 2016 09:44:39

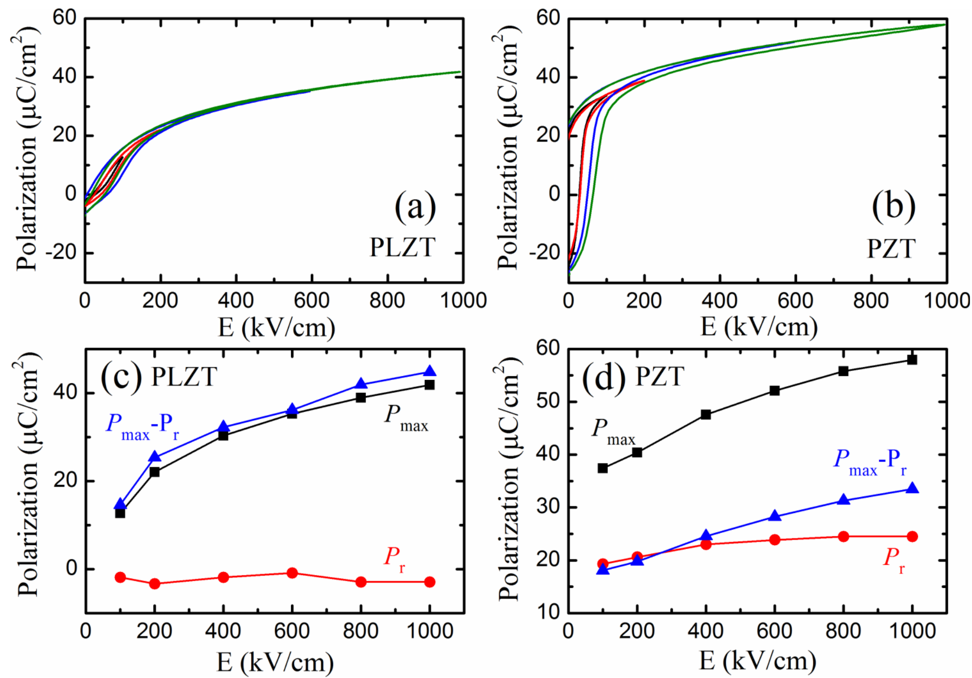

FIG. 3. Positive P-E hysteresis loops of (a) PLZT and (b) PZT thin films, under various electric fields and 1 kHz frequency. (c) and (d) The corresponding P_{max}, P_r, and ($P_{max} - P_r$) values of PLZT and PZT thin films.

and 88.2%, indicating a good stability; while the η value of PZT film increases by more than a factor 2 from 24.9% to 56.4%.

The U_{reco} and η values for the epitaxial relaxor-ferroelectric PLZT thin film in this study were 13.7 J/cm^3 and 88.2% at 1000 kV/cm, respectively, which is similar to the values measured for the antiferroelectric (AFE) films and much higher than in the polycrystalline relaxor ferroelectrics (RFE) listed in Table I. The higher energy storage performance of our epitaxial PLZT films for the same applied electric field, in comparison to the values of other reported relaxor-ferroelectric polycrystalline films (sol-gel $Pb_{0.92}La_{0.08}(Ti_{0.52}Zr_{0.48})O_3$ film on Pt/Si with U_{reco} = 9.8 J/cm^3 and η = 55.0%[7] and with U_{reco} = 12.8 J/cm^3 and η = 78.0%[6]) can be attributed to the fact that the P-E loop of our epitaxial PLZT/SRO/Si thin film sample is much narrower (and slightly pinched at

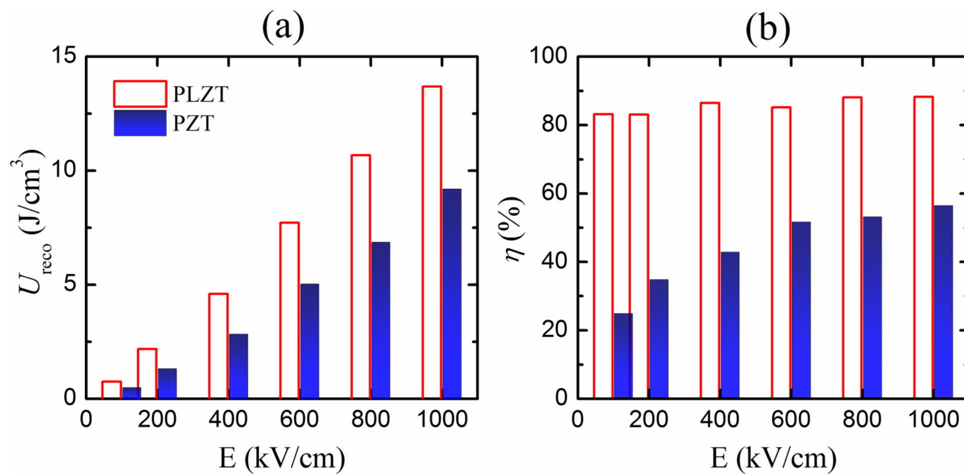

FIG. 4. (a) Recoverable energy storage density (U_{reco}) and (b) energy efficiency (η), of PLZT and (b) PZT thin films, as a function of maximum applied electric field, measured at 1 kHz frequency.

Reuse of AIP Publishing content is subject to the terms at: https://publishing.aip.org/authors/rights-and-permissions. Download to IP: 130.89.45.232 On: Wed, 05 Oct 2016 09:44:39

TABLE I. The recoverable energy storage density (U_{reco}) and energy storage efficiency (η) of antiferroelectric and relaxor ferroelectric thin films on Si substrates.

Films[a]	Film thickness (μm)	Substrate	Fabrication technique	U_{reco} (J/cm^3)	η (%)	E_{appl} (kV/cm)	References
(AFE) $Pb_{0.97}Y_{0.02}[(Zr_{0.6}Sn_{0.6})_{0.925}Ti_{0.075}]O_3$	0.5	Pt/Si	PLD	14.6	91.3	1000	2
(AFE) $(Pb_{0.95}Sr_{0.05})ZrO_3$	0.5	Pt/Si	Sol-gel	14.5	78.0	900	3
(RFE) $Pb_{0.91}La_{0.09}(Ti_{0.65}Zr_{0.35})O_3$	1	Pt/Si	Sol-gel	11.5	52.5	1000	5
(RFE) $Pb_{0.92}La_{0.08}(Ti_{0.52}Zr_{0.48})O_3$	1	Pt/Si	Sol-gel	9.8	55.0	1000	7
(RFE) $Pb_{0.92}La_{0.08}(Ti_{0.52}Zr_{0.48})O_3$	0.69	Pt/Si	Sol-gel	13	78	1000	6
				30	73	2200	
(RFE) $BaTiO_3/Ba_{0.3}Sr_{0.7}TiO_3$[b]	0.6	MgO	PLD	12.2	n.a.	1650	8
(RFE) $Pb_{0.9}La_{0.1}(Zr_{0.52}Ti_{0.48})O_3$	0.3	STO/Si	PLD	13.7	88.2	1000	This study
(RFE) $Pb_{0.9}La_{0.1}(Zr_{0.52}Ti_{0.48})O_3$	0.3	CeO_2/YSZ/Si	PLD	11.5	75.2	1000	This study
(FE) $Pb(Zr_{0.52}Ti_{0.48})O_3$	0.3	STO/Si	PLD	9.2	56.4	1000	This study

[a]AFE—Antiferroelectric; RFE—Relaxor ferroelectric; FE—–Ferroelectric.
[b]Superlattice.

low fields), decreasing the loss, and second because the loop is shifted in the field direction, thus increasing the stored energy. The effect of this on the U_{reco} and η values was investigated by growing a similar 300 nm thick, epitaxial (001)-oriented PLZT device on a CeO_2/YSZ buffered Si wafer. Fig. S4 compares the *P*-*E* loops of PLZT films grown on SRO/STO/Si and SRO/CeO_2/YSZ/Si substrates. The loop of the latter device does also show some pinching, as well as a self-bias field. The main differences are the significantly larger hysteresis and the slightly shallower slope of the loop. The SRO/PLZT//SROCeO$_2$/YSZ/Si exhibits a somewhat lower U_{reco} (11.5 J/cm^3) and η (75.2%) values than the SRO/L10ZT/SRO/STO/Si devices at 1000 kV/cm. The decrease in both U_{reco} and η values in PLZT film on CeO_2/YSZ/Si arises from the larger hysteresis (larger P_r and width of the hysteresis) and a less asymmetric *P*-*E* loop (less self-bias).

Electrical breakdown occurs in our devices for voltages somewhat above 1000 kV/cm, therefore we measured the energy density of our devices up to this value. This maximum electrical field value compares well with those given for similar devices on a Si substrate (see Table I). Higher field values and associated recoverable energy storage energies were quoted for a chemical solution deposited film of Ref. 6 and for the multilayer device of Ref. 8. None of the latter studies give a statistical spread of the breakdown voltage of these devices, thus it is unclear if these are typical or best values. We have used the value of 1000 kV/cm as the maximum applied field also for easy quantitative comparison with other devices.

Fig. 5 gives the electrical polarization fatigue behavior of the PLZT thin films on STO/Si substrates as a function of the number of switching cycles up to 10^{10} cycles. The schematic of bipolar, positive unipolar, and negative unipolar fatigue signals is shown in Fig. S5. Fig. 5(a) shows that both P_r and P_{max} values increase with the number of bipolar fatigue cycles. It is seen in Fig. 6(a) that the *P*-*E* loop shifts slightly to the left (smaller self-bias voltage). Further the maximum polarization value increases somewhat. The bipolar effect of the cycling is that U_{reco} and U_{store} values are reduced by about 4%-5%, but only little change of efficiency is observed (Fig. 5(b)). Under unipolar cycling, P_{max} decreases significantly, whereas the remanent polarization values approach zero (Figs. 6(b) and 6(c)). The latter is not due to a narrower hysteresis loop but due to a decreasing self-bias field. U_{reco} and U_{store} values are significantly reduced for both positive and negative unipolar cycling by up to 23%. The efficiency increases with cycling and saturates with an increase of as much as 7.4% for positive unipolar cycling because the enclosed area of the *P*-*E* loop is reduced, while for the negative unipolar cycling, the efficiency remains approximately constant within 2.7%. The change of the *P*-*E* loops of the PLZT loops upon cycling indicates that the charge distribution in the film is slowly rearranged depending on the polarity of the cycling, changing the net polarization. For every two La doping ions, one expects one Pb vacancy to be present to maintain charge neutrality,[15] hence for 10% La doping this would imply a 5% V_{Pb} density. Next to the not very mobile Pb

Reuse of AIP Publishing content is subject to the terms at: https://publishing.aip.org/authors/rights-and-permissions. Download to IP: 130.89.45.232 On: Wed, 05 Oct 2016 09:44:39

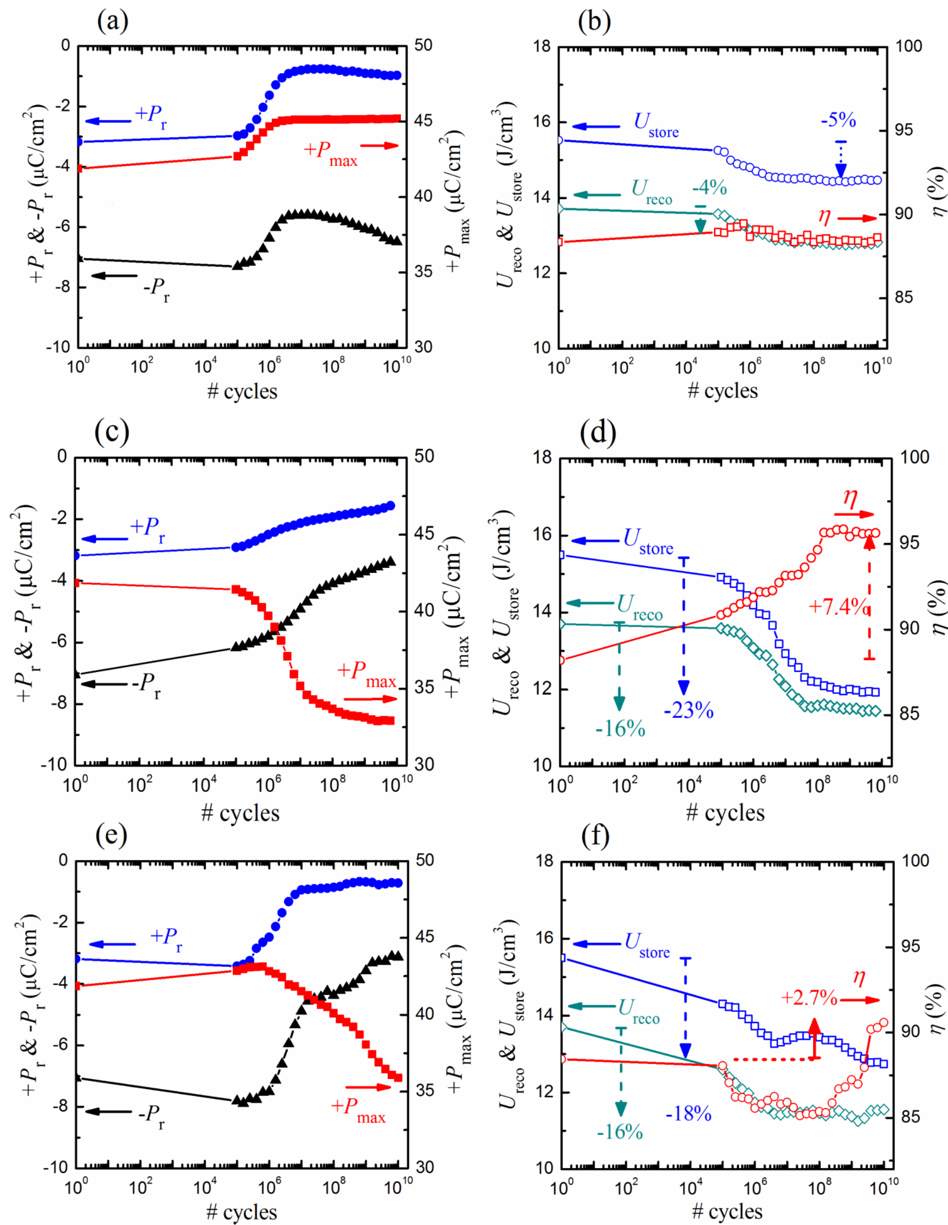

FIG. 5. Remanent polarization ($+P_r$ and $-P_r$) and positive maximum polarization ($+P_{max}$); recoverable energy density (U_{reco}), energy storage (U_{store}), and energy efficiency (η) with (a) and (b) bipolar fatigue at 200 kV/cm, (c) and (d) positive unipolar at +200 kV/cm, and (e) and (f) negative unipolar at −200 kV/cm, as a function of the number of switching cycles up to 10^{10} cycles, for PLZT films on SRO/STO/Si. These values were obtained from P-E loops measured up to ±1000 kV/cm at 1 kHz frequency.

vacancies, a significant number of very mobile oxygen vacancies are always present. A fraction of these charged defects rearrange under the influence of an applied field forming dipoles. Under a bipolar switching field, we observe a small increase of the maximum polarization (see Fig. 5(a)), indicating the formation or field alignment of switchable dipoles. Under a unipolar switching field, P_{max} is significantly reduced, indicating that a fraction of the switchable dipoles becomes pinned by the local field of displaced charges. Further there is an asymmetry in the positive and negative polarity cycling response. For positive polarity, P_{max} drops much quicker than for negative polarity, indicating a difference in mobile charge mobility in upward and downward direction. The polarizations of the PZT films are hardly affected by cycling, see Fig. S6(a), hence U_{store}, U_{reco}, and η values remain unchanged with the number of cycles, see Fig. S6(b).

Reuse of AIP Publishing content is subject to the terms at: https://publishing.aip.org/authors/rights-and-permissions. Download to IP: 130.89.45.232 On: Wed, 05 Oct 2016 09:44:39

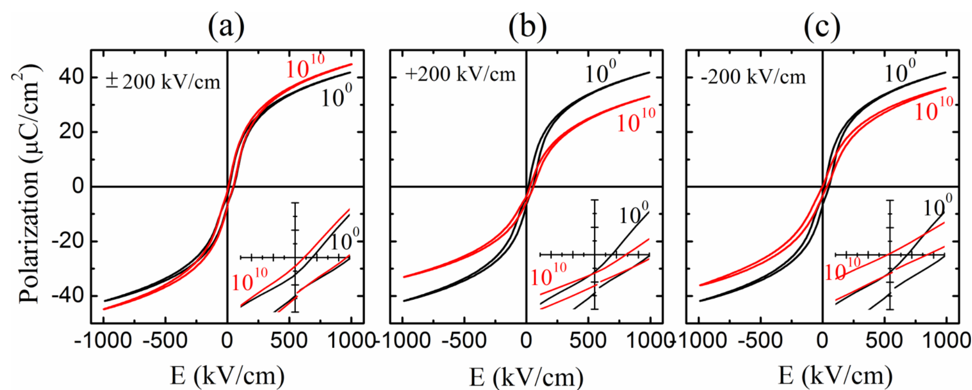

FIG. 6. (a) Bipolar fatigue, (b) positive unipolar fatigue, and (c) negative unipolar fatigue evaluated by P-E hysteresis loops of PLZT film on SRO/STO/Si, after 1 and 10^{10} cycles.

In summary, we fabricated (001)-oriented epitaxial PZT ferroelectric and 10% La doped epitaxial PLZT relaxor-ferroelectric thin films on SRO/STO/Si substrates using pulsed laser deposition. A large recoverable energy storage density of 13.7 J/cm^3 and a high energy efficiency of 88.2% (measured at a maximum electric field of 1000 kV/cm and at 1 kHz) were obtained in the PLZT film. The values for these epitaxial thin films are very well comparable with the best values reported in the literature obtained in antiferroelectric thin films and are significantly larger than for sol-gel deposited thin films. These properties demonstrate that epitaxial PLZT relaxor-ferroelectric thin films are promising for application in high power energy storage devices.

See supplementary material for the schematic polarization-electric field (P-E) loops of dielectric, ferroelectric, relaxor ferroelectric, and antiferroelectric materials; typical dependence of the polarization on positive electric field for a relaxor ferroelectric material; bipolar P-E hysteresis loops of epitaxial $Pb_{0.9}La_{0.1}(Ti_{0.52}Zr_{0.48})O_3$ (PLZT) and $Pb(Ti_{0.52}Zr_{0.48})O_3$ (PZT) thin films, grown on SRO/STO/Si; XRD pattern of epitaxial PLZT film grown on SRO/CeO_2/YSZ/Si and bipolar ferroelectric P-E hysteresis loops of the epitaxial PLZT thin films grown on SRO/STO/Si and SRO/CeO_2/YSZ/Si; schematic of bipolar, positive unipolar, and negative unipolar fatigue signal profiles; remanent polarization and positive maximum polarization, and recoverable energy density, energy storage, and energy efficiency with bipolar fatigue at 200 kV/cm, as a function of switching cycles up to 10^{10}, of PZT film on SRO/STO/Si.

This work is financially supported by the Vietnamese MOET Science and Technology Research Program under Grant No. B2014-01-62, and by the NanoNextNL, a micro and nanotechnology consortium of the Government of the Netherlands and 130 partners.

[1] N. H. Fletcher, A. D. Hilton, and B. W. Ricketts, J. Phys. D: Appl. Phys. **29**, 253 (1996).
[2] C. W. Ahn, G. Amarsanaa, S. S. Won, S. A. Chae, D. S. Lee, and I. W. Kim, ACS Appl. Mater. Interfaces **7**, 26381 (2015).
[3] X. Hao, J. Zhai, and X. Yao, J. Am. Ceram. Soc. **9**, 1133 (2009).
[4] Y. Wang, X. Hao, J. Yang, J. Xu, and D. Zhao, J. Appl. Phys. **112**, 034105 (2012).
[5] X. Hao, Y. Wang, J. Yang, S. An, and J. Xu, J. Appl. Phys. **112**, 114111 (2012).
[6] Z. Hu, B. Ma, S. Liu, M. Narayanan, and U. Balachandran, Ceram. Int. **40**, 557 (2014).
[7] S. Tong, B. Ma, M. Narayanan, S. Liu, R. Koritala, U. Balachandran, and D. Shi, ACS Appl. Mater. Interfaces **5**, 1474 (2013).
[8] N. Ortega, A. Kumar, J. F. Scott, D. B. Chrisey, M. Tomazawa, S. Kumari, D. G. B. Diestra, and R. S. Katiyar, J. Phys.: Condens. Matter **24**, 445901 (2012).
[9] C. Marchiori, M. Sousa, A. Guiller, H. Siegwart, J.-P. Locquet, J. Fompeyrine, G. J. Norga, and J. W. Seo, Appl. Phys. Lett. **88**, 072913 (2006).
[10] M. D. Nguyen, E. Houwman, M. Dekkers, H. N. Vu, and G. Rijnders, Sci. Adv. Mater. **6**, 243 (2014).
[11] H. Funakubo, M. Dekkers, A. Sambri, S. Gariglio, I. Shklyarevskiy, and G. Rijnders, MRS Bull. **37**, 1030 (2012).
[12] S. Tong, M. Narayanan, B. Ma, S. Liu, R. E. Koritala, U. Balachandran, and D. Shi, Mater. Chem. Phys. **140**, 427 (2013).
[13] S. J. Kang and Y. H. Joung, J. Mater. Sci. **42**, 7899 (2007).
[14] M. Boota, E. P. Houwman, M. Dekkers, M. Nguyen, and G. Rijnders, Appl. Phys. Lett. **104**, 182909 (2014).
[15] B. Jaffe, W. R. Cook, Jr., and H. Jaffe, *Piezoelectric Ceramics* (Academic, Press, London, 1971), p. 146.

Reuse of AIP Publishing content is subject to the terms at: https://publishing.aip.org/authors/rights-and-permissions. Download to IP: 130.89.45.232 On: Wed, 05 Oct 2016 09:44:39